

## THERMAL EXPERIMENTAL AND NUMERICAL HEAT TRANSFER ANALYSIS OF A SOLID CYLINDER IN LONGITUDINAL DIRECTION

*<sup>1</sup>Sebastian Cabezas, <sup>1</sup>György Hegedűs, <sup>1</sup>Péter Bencs*

<sup>1</sup>University of Miskolc, Department of Machine Tools and Department of Fluid and Heat Engineering, Miskolc-Egyetemváros, HU-3515, Miskolc-Hungary

e-mail: szgtscab@uni-miskolc.hu, hegedus.gyorgy@uni-miskolc.hu, peter.bencs@uni-miskolc.hu

### ABSTRACT

The analysis of heat transfer in solid bodies with orthogonal geometries and knowledge thereof, is of vast importance in different fields of engineering and research. An important field of study is the thermal analysis in machine-parts that in most cases are designed and shaped with orthogonal geometries. Nevertheless, due to the high complexity and the cost that thermal experiments represent, FEM analysis and numerical solutions are used to foresee thermal fields on these components. These methodologies are certainly reliable, although may vary from real experiments. On that account, this paper presents a thermal experimental test in a solid cylinder of length  $l_T = 168$  mm and  $\varnothing = 33$  mm, made of C45 steel that emulates a machine-part (cylindrical parts as shafts, fasteners and the like). The temperature fields along the longitudinal direction  $z$  were analyzed in steady and transient state under homogeneous boundary conditions of the first kind (prescribed temperatures at the boundaries). The three solutions, experimental, numerical solution by finite difference method and FEM simulations in steady and transient state were compared with the purpose of validating the results obtained by each method of solution. It could be seen that the maximum mean deviation was  $s = 0.53$  and  $s = 0.44$  for steady and transient state respectively, herewith proving that by the three solutions under the established boundary conditions can be applied individually.

Keywords: Orthogonal geometries, temperature fields, steady and transient state, Numerical solutions, FEM analysis.

### 1. INTRODUCTION

The determination of the temperature fields in solid bodies with orthogonal geometries has been tackled by many researchers throughout the time. Different ways and methodologies have been applied in order to predict and obtain reasonable results that are adaptable to real thermal problems. Among these methodologies are the analytical solutions of the heat conduction equation, FEM (Finite Element Method) simulations and the prediction of the temperature distribution by other numerical methods such as finite difference method.

Although these techniques provide an appropriate prediction and clear knowledge of the temperature fields, it is needed to adapt these solutions to reality. However, due to the complexity and costs that the implementation of thermal experimental rigs represent, in most cases, simulations and analytical solutions are the only way to determine the temperature distribution. The reason to obtain the temperature fluctuations in solid bodies must be sustained in real applications, such as industrial, engineering or research & development that contribute with important solutions in the field of heat transfer. To illustrate, Kadhim D., et. al., performed an analytical evaluation to determine the temperature dependent thermal conductivity in a hollow cylinder with three different types of metallic materials [1], thus showing how the thermal conductivity of the material will fluctuate with temperature variations. Another important research field is thermal analysis in machine-tools and machine-parts. Several unsatisfactory effects e.g., tool-misalignment, wear of machine components, machining errors, energy losses, wrong machine tool's manufacturing accuracy and the like are occasioned due to thermal deformations [2]. Machine-parts, such as shafts, bearings, sealings, fasteners, housings, together with further mechanical components that are part of the machine-tool assembly, are subjected to heat dissipation due to power losses that occur by the interaction between the internal and external energy sources which are involved in a machining or mechanical process. The sudden increase of temperature or the prolonged temperature fluctuations in a machine-part may cause irreversible thermal deformations. It's been analyzed by some researchers, e.g.

[3,4,5,10], that determining experimentally the temperature fields in a machine-tool is complicated in view of the fact that accessing in the inner parts, e.g., shafts, bearings either is not possible or requires assembly modifications, thereby causing damage or failure in the machine-tool. Nevertheless, knowing that most of the inner components of a machine-tool have orthogonal geometries, an individual thermal analysis thereof, under specific boundary and initial conditions can be performed over a solid geometry with similar thermal properties and the obtained experimental values can be applied in thermal simulations, thus predicting more accurate results in the analysis without affecting a machine-part. Further studies have been performed related with thermal analysis in cylindrical geometries can be found in [11,13] wherein effects of heat by convection are studied experimentally.

On that account, this paper presents a thermal experimental and analytical test in a solid cylinder of length  $l_T = 168$  mm and  $\varnothing = 33$  mm, made of C45 steel that emulates a machine-part (cylindrical component) with the aim to validate the numerical and FEM simulations simultaneously. The heat conduction analysis was carried out along the longitudinal direction  $z$  in steady and transient state under homogeneous boundary conditions of the first kind (prescribed temperature). The heating source was provided by an electrical heater of power capacity  $P = 1500$  W. Power losses transferred from an electrical motor to a mechanical component by conduction, can be dissipated in the form of heat in the longitudinal, angular and radial directions through the body [6]. The results show the validity of the numerical and FEA simulations which can be applied for future works without the need to perform successive experiments in parts of similar geometry subjected to boundary conditions of the first kind.

## 2. HEAT TRANSFER ANALYSIS IN A SOLID CYLINDER

The thermal analysis in the present work was performed solving the 1-D heat conduction equation in the longitudinal direction  $z$  for a solid cylinder with prescribed temperature at the boundaries (boundary conditions of the first kind). The determination and classification of boundary conditions can be found in [12,14,15]. The analysis is divided into three parts. In the first part, the solution of the heat conduction equation is obtained by applying numerical solutions, the second part involves the application of FEM thermal analysis using Ansys, finally, the implementation of the thermal experimental rig is carried out in the third part.

### 2.1. Numerical Solution of the 1-D Heat Conduction Equation in steady and transient state.

The numerical solutions of the 1-D heat conduction equation of a solid cylinder in steady and transient state were obtained by applying the finite difference method. Fig.1, illustrates the geometry of application. The finite difference method is a versatile numerical method that has been widely used for the solution of partial differential equations of heat and mass transfer [7].

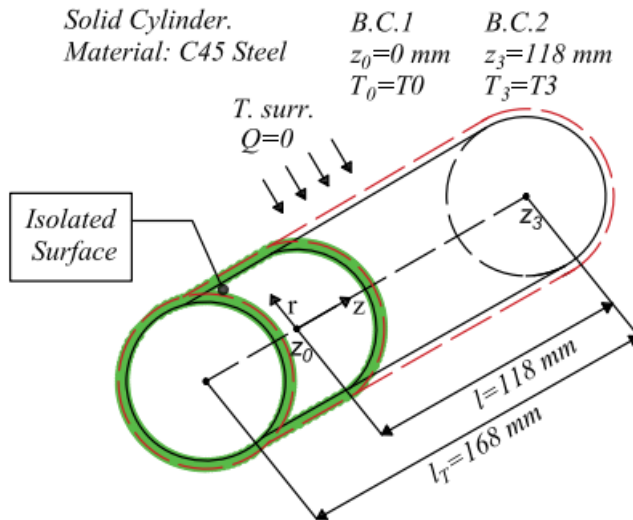


Figure 1. Heat Conduction in a solid cylinder with prescribed temperature in longitudinal direction  $z$ .

### 2.1.1 1-D Heat Transfer in Steady-state. Finite Difference Solution.

In steady-state, the heat conduction equation for a solid cylinder in longitudinal direction  $z$  is stated as

$$\begin{cases} k \frac{\partial^2 T}{\partial z^2} = 0 \\ T_0 = T_0, T_3 = T_3 \end{cases} \quad (1)$$

Where  $k$  is the thermal conductivity. The boundary conditions  $T_0$  and  $T_3$  are prescribed temperatures at the position  $z = 0$  mm and  $z = 118$  mm respectively.

Equation 1 is solved using the finite difference approximation of the second order. The solid cylinder is divided into small sections  $\delta_z$  and in  $m$  number of nodal points as shown in Fig. 2.

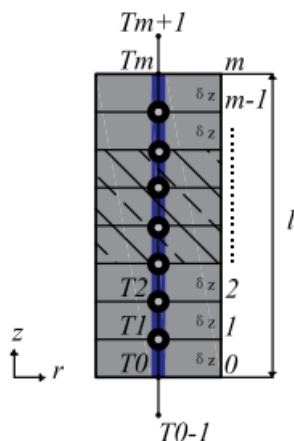


Figure 2. Finite difference approximation in the  $z$  direction of a solid cylinder.

$$k \cdot \frac{T_{i-1} - 2T_i + T_{i+1}}{\delta z^2} = 0 \text{ for } i = 1, 2, 3, \dots, m - 1 \quad (2)$$

$$T_{m=0} = T_0, T_{m=1} = T_3$$

The matrix solution is expressed as

$$\begin{bmatrix} 1 & 0 & 0 & 0 \\ 1 & -2 & 1 & 0 \\ 0 & 1 & -2 & 1 \\ 0 & 0 & 0 & 1 \end{bmatrix} \begin{bmatrix} T_0 \\ T_1 \\ T_2 \\ T_3 \end{bmatrix} = \begin{bmatrix} T_0 \\ 0 \\ 0 \\ T_3 \end{bmatrix} \quad (3)$$

### 2.1.2 1-D Heat Transfer in Transient-state. Finite Difference Solution.

In transient state, the heat conduction equation for a solid cylinder in longitudinal direction  $z$  is stated as

$$\begin{cases} k \frac{\partial^2 T}{\partial z^2} = \rho c_p \frac{\partial T}{\partial t} \\ T(0, t) = T_0, T(l, t) = T_3 \quad t > 0 \\ T(z, 0) = F(z) \quad t = 0 \end{cases} \quad (4)$$

Where  $k$  is the thermal conductivity,  $\rho$  is the density of the material,  $c_p$  is the specific heat of the material. The initial condition is a temperature function  $F(z)$  that depends on the position  $z$ .

Equation 4 is solved using the finite difference approximation of the second order for the displacement dependent variable (left side of the energy equation) and the time dependent variable (right side of the equation) is solved using the finite difference approximation of the first order.

$$\frac{T_{i-1}^n - 2T_i^n + T_{i+1}^n}{\delta z^2} = \frac{1}{\alpha} \frac{T_i^{n+1} - T_i^n}{\delta t}$$

$$\frac{\alpha \cdot \delta t}{\delta z^2} \cdot (T_{i-1}^n - 2T_i^n + T_{i+1}^n) = T_i^{n+1} - T_i^n$$

Equation 4 in terms of finite difference approximation is stated as

$$\begin{cases} T_i^{n+1} = p \cdot T_{i-1}^n + (1 - 2p) \cdot T_i^n + p \cdot T_{i+1}^n \\ T_0^n = T_0, T_m^n = T_3 \\ T_m^0 = F(z) \end{cases} \quad (5)$$

Where  $p = \frac{\alpha \delta t}{\delta z^2}$ ,  $i = 1, 2, 3, \dots, m - 1$  and the time intervals  $n = 1, 2, 3, \dots$

It is important to mention that numerical and analytical solutions of the transient heat conduction equation are stable for small intervals of time, called short co-times [8].

## 2.2. Finite Element Method.

To date, professional FEM software packages support engineers and researchers in the field of thermal analysis. Although the solutions are certainly reliable, fast and in a sense simple to obtain, may vary from reality. Therefore, the FEM simulations must be compared either analytically or experimentally. In this work, FEM thermal analysis was performed for a solid cylinder using ANSYS in steady and transient state. The results of the simulations were compared with the numerical and the experimental approach. The results can be seen in section 3 (Results and Discussion).

## 2.3. Experimental thermal analysis.

A cylindrical test probe made of C45 steel with thermal conductivity  $k = 40 - 45 \frac{W}{mmK}$ , specific heat capacity  $c_p = 460 - 480 \frac{J}{kg \cdot K}$  and density  $\rho = 7.8 \cdot 10^{-6} \frac{kg}{mm^3}$  was used to determine the temperature fields in steady and transient state. The test probe made of C45 steel was selected based on the fact that this type of material is widely used in the manufacturing of machine-parts for its good torsional strength and fatigue resistance [9]. The heat isolator 1, made of polystyrene, with thermal conductivity  $\lambda_1 = 3.3 \cdot 10^{-5} \frac{W}{mmK}$ , is used to avoid heat transfer by convection between the surroundings of the experimental rig and the test probe. Due to the low thermal conductivity of polystyrene, temperature fluctuations that might distort the measurements are evaded. The heat isolator 2, made of autoclaved aerated concrete with thermal conductivity  $\lambda_2 = 1.3 \cdot 10^{-5} \frac{W}{mmK}$  was used to avoid heat transfer between the heat source and the solid cylinder either by convection when the heated air flows up and surrounds the surface of the cylinder or by radiation occasioned by the heated plate. The heat source with nominal power  $P = 1500 W$ , was used to transfer heat in the longitudinal direction  $z$ . A steel plate is located between the power source and the test probe to level the surfaces of the cross-sectional face of the solid cylinder and the power source. A 4-channel data logger thermometer was used to obtain the measurements of 4 type T-thermocouples connected on the surface of the solid cylinder. Fig. 3 a), shows the parts and components of the experimental rig and Fig.3 b), the position of the type T-thermocouples.

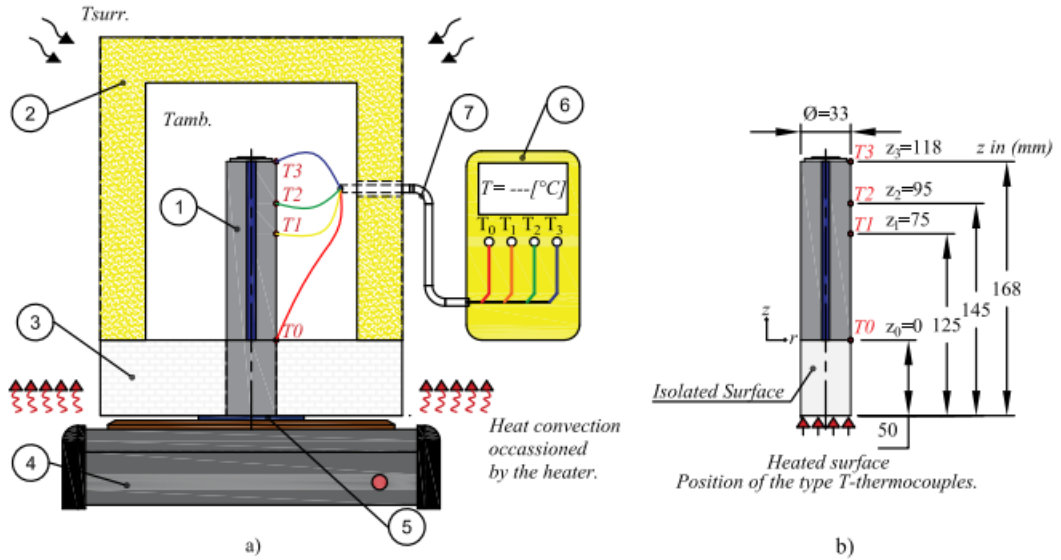


Figure 3. a) Experimental Rig, b) Position of the thermocouples Type-T

A detailed description of the parts and components of the experimental rig are described in Table 1.

Table 1. Parts and components of the experimental rig.

Symbol	Parameter	Units	Characteristics
1	Test Probe	1	Material: C45 steel. $l = 118 \text{ mm}$ $\varnothing = 33 \text{ mm}$
2	Heat Isolator 1	1	Material: Polystyrene $h = 30 \text{ mm}$ , $\lambda_1 = 3.3 \cdot 10^{-5} \frac{\text{W}}{\text{mmK}}$
3	Heat Isolator 2	1	Material: Autoclaved aerated concrete $w = 200 \text{ mm}$ , $d = 200 \text{ mm}$ $h = 50 \text{ mm}$ , $\lambda_2 = 1.3 \cdot 10^{-5} \frac{\text{W}}{\text{mmK}}$
4	Heat Source	1	Nominal Power $P = 1500 \text{ W}$
5	Steel Plate	1	$w = 70 \text{ mm}$ , $d = 50 \text{ mm}$ , $h = 2 \text{ mm}$
6	Data Logger Thermometer	1	YCT YC-747D. Range: T – Thermocouple ( $-100 \text{ }^\circ\text{C} - 400 \text{ }^\circ\text{C}$ ) Accuracy: $\pm (0.1 \% \text{ rdg.} + 0.7 \text{ }^\circ\text{C})$ Resolution: $0.1 \text{ }^\circ\text{C}$ LCD update: 1 per second
7	Temperature Sensors	4	Type T-Thermocouples Range: ( $-100 \text{ }^\circ\text{C} - 400 \text{ }^\circ\text{C}$ )

The parts and components of the experimental rig were assembled in accordance with the diagram shown in Fig. 3 a).

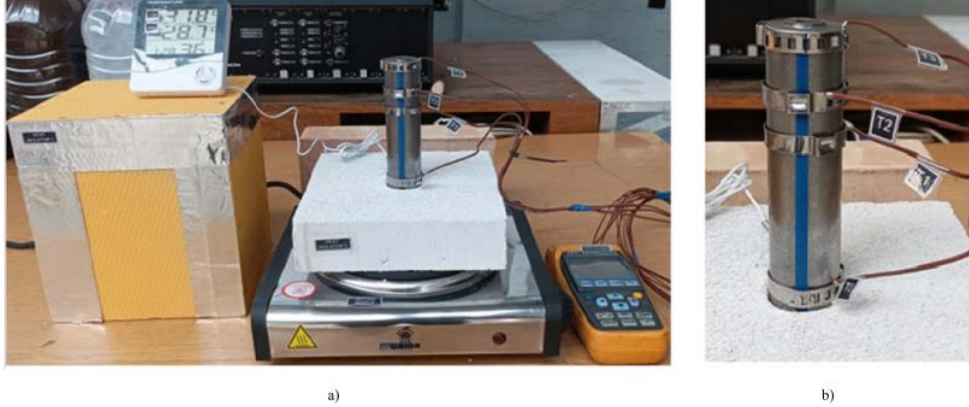


Figure 4.a) Implementation of the Experimental Rig, b) Connection of the type T-thermocouples.

### 3. RESULTS AND DISCUSSION

A comparison among finite difference method, FEM simulations, and experimental analysis was carried out to determine the temperature distribution in steady and transient state.

#### 3.1 Steady State Analysis

The temperature distribution in steady state along the longitudinal direction  $z$  in the test probe was obtained by several experimental measurements. Tab. 2 presents an excerpt of 3 experimental measurements from nearly 70, which were compared with the numerical and FEM solutions.

Table 2. Experimental measurements in steady state.

Measurement Instrument: Thermometer YCT YC-747D						
Thermocouple range: Type T thermocouple (−100 °C to 400 °C)						
Accuracy: $\pm(0.1 \% \text{ rdg.} + 0.7 \text{ }^\circ\text{C})$						
Resolution: 0.1 °C						
LCD update: 1 per second.						
Experiment	$T_0, (^\circ\text{C})$	$T_1, (^\circ\text{C})$	$T_2, (^\circ\text{C})$	$T_3, (^\circ\text{C})$	$T_{\text{amb.}}, (^\circ\text{C})$	$T_{\text{surr.}}, (^\circ\text{C})$
	$z = 0$	$z = 75$	$z = 95$	$z = 118$	-	-
1	36.10	33.90	33.70	33.50	30.70	30.70
2	37.50	35.50	35.70	35.40	31.60	30.80
3	54.10	49.10	49.50	48.50	36.70	30.00

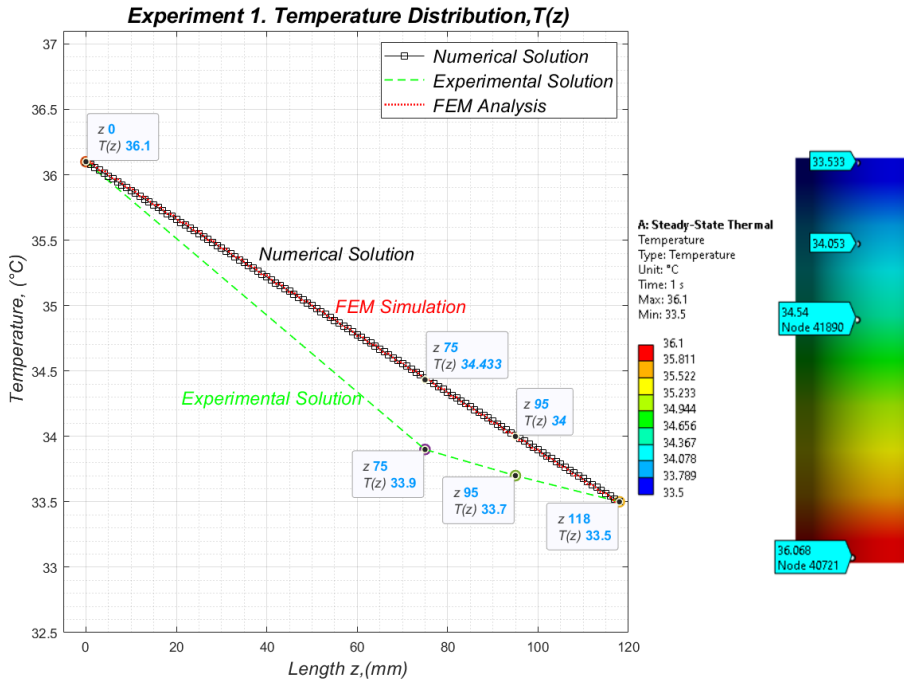


Figure 5. Temperature Distribution in steady state. B. C. 1  $\rightarrow T_0 = 36.1$  °C, B. C. 2  $\rightarrow T_3 = 33.5$  °C

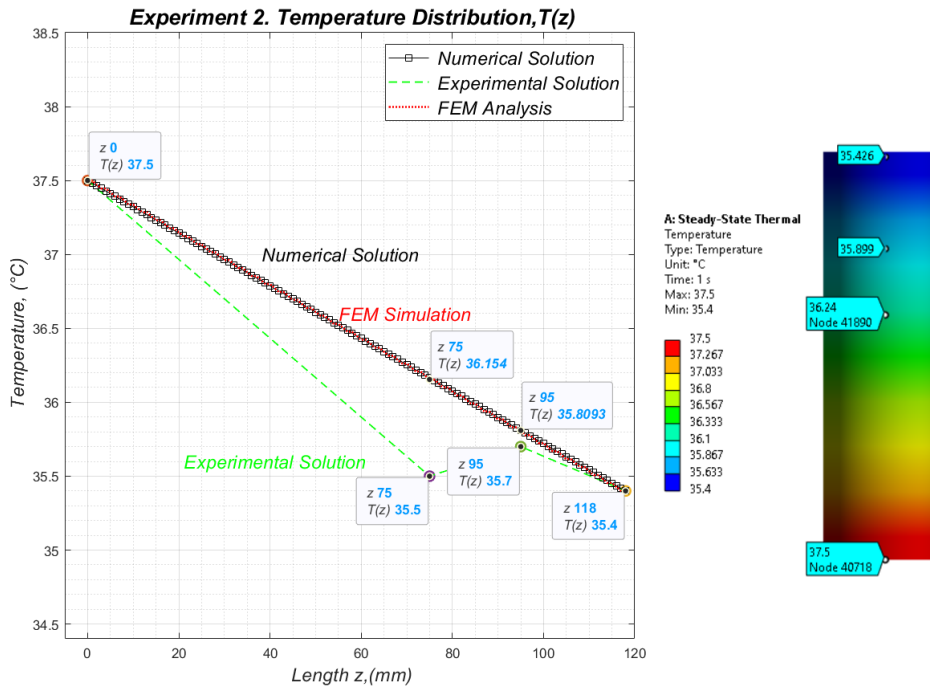


Figure 6. Temperature Distribution in steady state. B. C. 1  $\rightarrow T_0 = 37.5$  °C, B. C. 2  $\rightarrow T_3 = 35.4$  °C

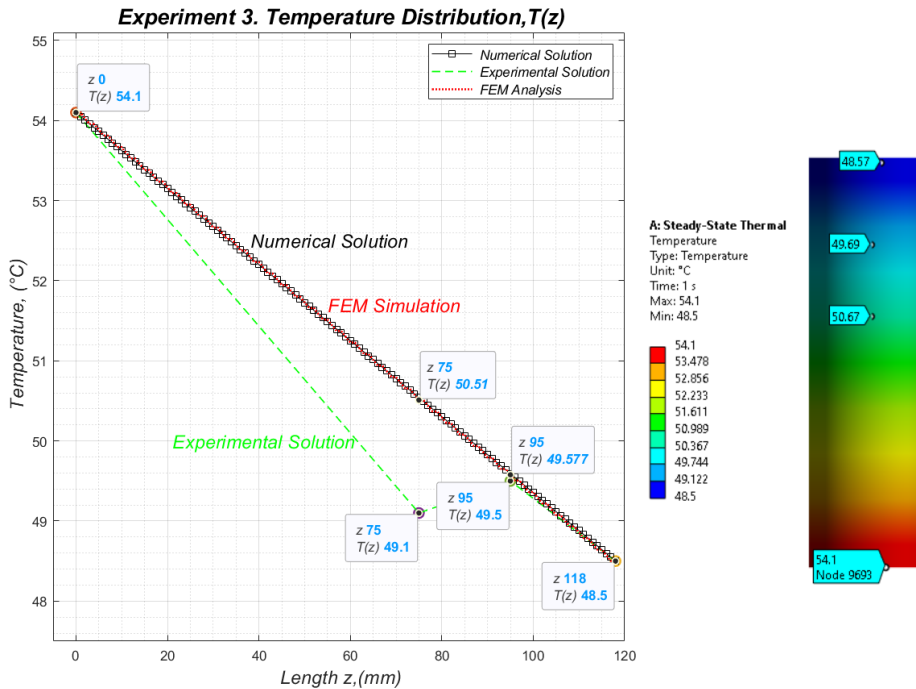


Figure 7. Temperature Distribution in steady state. B. C. 1  $\rightarrow T_0 = 54.1\text{ }^\circ\text{C}$ , B. C. 2  $\rightarrow T_3 = 48.5\text{ }^\circ\text{C}$

To validate the solutions, the mean deviation among the experimental, numerical and FEM solutions was calculated. If these values do not vary more than specified accuracy of the sensor (0.1 % rdg. +0.7 °C), can be considered as appropriate. Table 3, presents the calculated values of the mean deviation.

Table 3. Mean deviation and data comparison of the thermal analysis in steady state.

Experiment	$T_{z=75} = T_1\text{ (}^\circ\text{C)}$				$T_{z=95} = T_2\text{ (}^\circ\text{C)}$			
	Meas.	F. D.	FEM	Dev.	Meas.	F. D.	FEM	Dev.
1	33.90	34.43	34.44	0.30	33.70	34.00	33.98	0.16
2	35.50	36.15	36.16	0.37	35.70	35.8	35.79	0.05
3	49.60	50.51	50.53	0.53	49.50	49.57	49.55	0.03

### 3.2. Transient State Analysis

The experimental measurements for transient-state analysis were obtained once the test probe started the process of natural cooling. A linear function considered as the initial condition  $T(z,0) = F(z)$  was constructed with 4 experimental measurements when the time was set up to be initial  $t = 0\text{ s}$ , starting the natural cooling process.

Table 4. Initial values of temperature for transient state analysis  $t = 0$ .

	$T_0, \text{ (}^\circ\text{C)}$	$T_1, \text{ (}^\circ\text{C)}$	$T_2, \text{ (}^\circ\text{C)}$	$T_3, \text{ (}^\circ\text{C)}$
$t = 0\text{ s}$	$z = 0\text{ mm}$	$z = 75\text{ mm}$	$z = 95\text{ mm}$	$z = 118\text{ mm}$
	56.80	55.50	56.40	56.00

Utilizing the data presented in Tab. 4, the initial function  $T(z, 0)$  is

$$T(z, 0) = -0.006 \cdot z + 56.633, \quad t = 0 \quad (6)$$

The values of the boundary conditions were set as  $T(z = 0, t) = 53.4 \text{ }^\circ\text{C}$  and  $T(z = 118, t) = 53.4 \text{ }^\circ\text{C}$  for all  $t > 0$ . To determine the thermal distribution and compare the values of the three different transient state solutions (experimental, finite difference method and FEM simulations), different measurements were obtained at  $t$  equals to 10, 20, 30, 60, 120, 300 and 480 s.

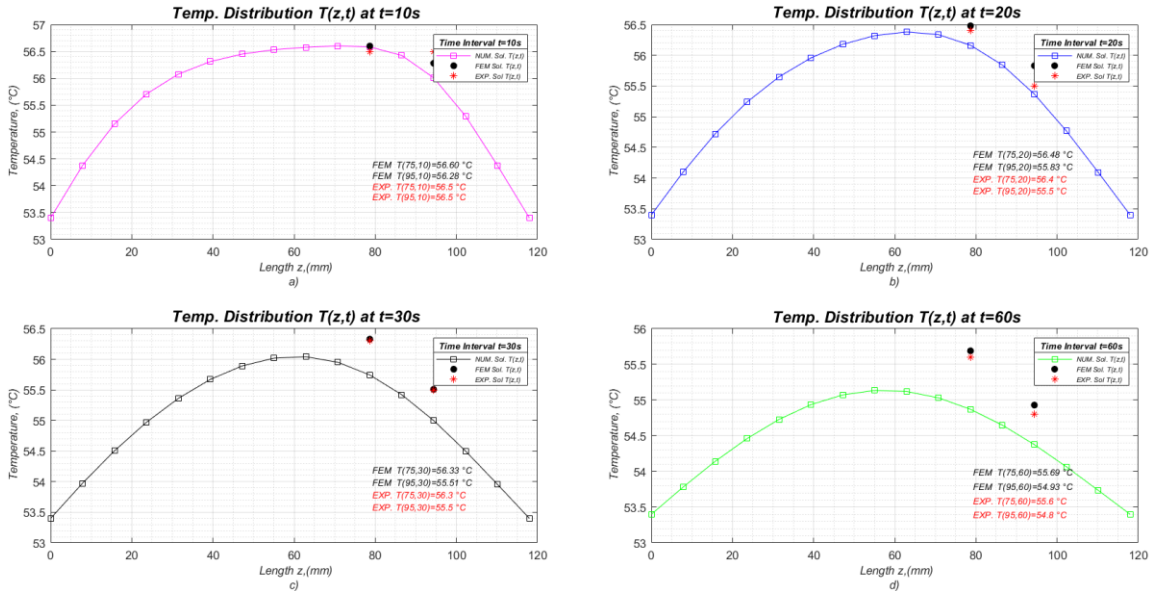


Figure 8. Transient state analysis a)  $\Delta t = 10$  s, b)  $\Delta t = 20$  s, c)  $\Delta t = 30$  s, d)  $\Delta t = 60$  s.

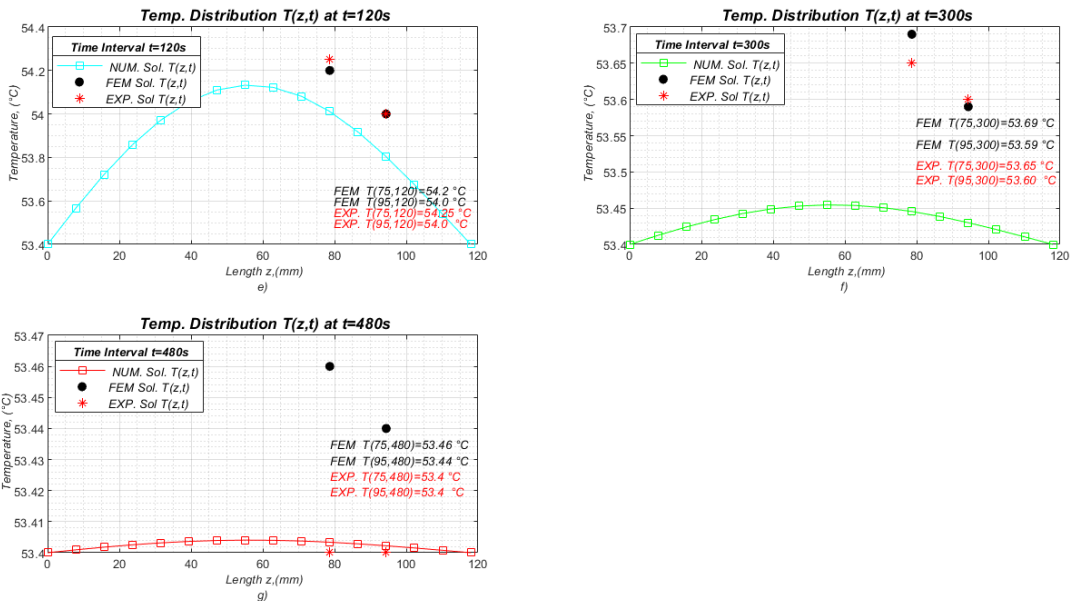


Figure 9. Transient state analysis e)  $\Delta t = 120$  s, f)  $\Delta t = 300$  s, g)  $\Delta t = 480$  s.

To validate the solutions, the mean deviation was calculated following the same procedure above mentioned for steady state analysis. The results are presented in Tab. 5.

*Table 5. Mean deviation and data comparison of the thermal analysis in transient state.*

time, (s)	z = 75 mm				z = 95 mm			
	Exp.	F. D.	FEM	Dev.	Exp.	F. D.	FEM	Dev.
10	56.50	56.58	56.60	0.05	56.50	56.00	56.28	0.25
20	56.40	56.16	56.48	0.16	55.50	55.36	55.83	0.24
30	56.30	55.74	56.33	0.33	55.50	54.99	55.31	0.25
60	55.60	54.87	55.69	0.44	54.80	54.37	54.93	0.29
120	54.25	54.01	54.20	0.12	54.00	53.80	54.00	0.11
300	53.65	53.44	53.69	0.13	53.60	53.43	53.60	0.09
480	53.40	53.40	53.46	0.03	53.40	53.40	53.44	0.02

The temperature variation against time was determined for the three solutions in consideration.

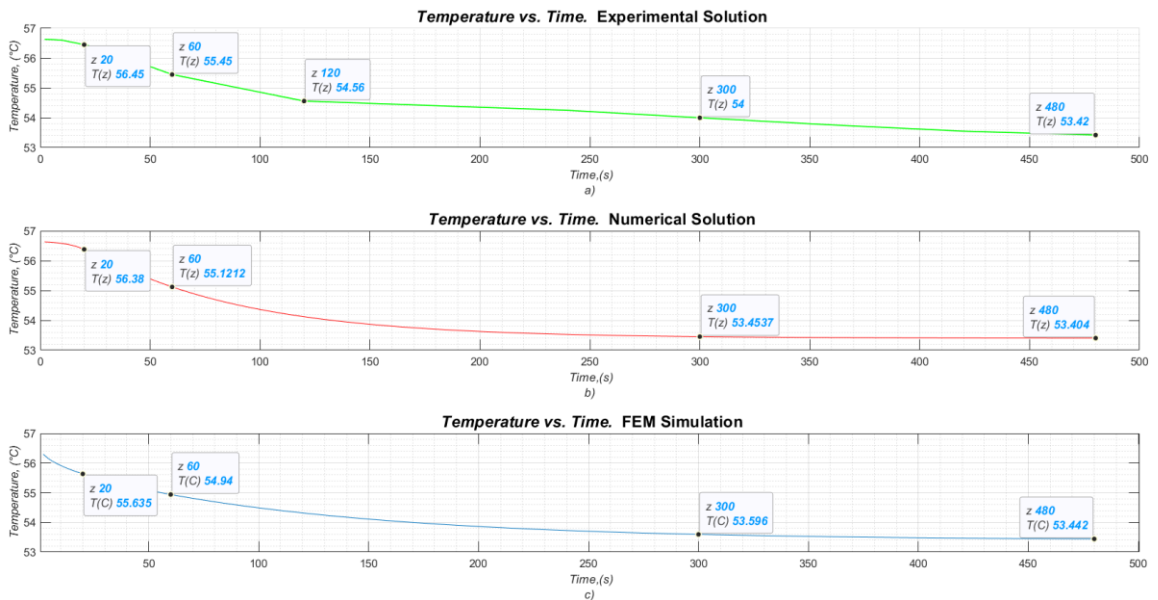


*Figure 10. Temperature vs. time, a) Exp. Solution, b) F.D. Solution, c) FEM.*

## 4. CONCLUSIONS

The solutions for steady and transient state under prescribed temperature boundary conditions were analyzed by three different methods of solution, experimental, numerical by finite difference method and by FEM simulations. The comparisons between the results were compared, thus the following conclusions are derived:

- Considering that many machining parts have cylindrical geometries, the individual analysis of orthogonal geometries as shown in this case, supports the validation of numerical and FEM simulations without the need to perform further experiments since this work supports sundry

experiments wherein the conditions are alike. The results can be applied in the development of thermal models evolving geometries alike.

- In steady state, the maximum mean deviation among the three solutions presented in this work was  $s = 0.53$ , since the value is under the accuracy limits of the temperature datalogger utilized in the experimental analysis.
- In transient state, the analysis was performed during  $t = 480$  s and various measurements were taken at different times shown in Tab. 5, The maximum mean deviation obtained was  $s = 0.44$ , hence the results are appropriate.

## REFERENCES

- [1] E. K. Dheyaa, H.K. Jobair & A.I. Oday, Analytical evaluation of temperature dependent thermal conductivity for solid and hollow cylinders subjected to a uniform heat generation. *International Journal of Mechanical Engineering and Technology*, vol.9 (10), October (2018), pp. 1095-1106.
- [2] K. Großman, *Thermo-energetic Design of Machine Tools*. Springer, (2015). DOI: 10.1007/978-3-319-12625-8.
- [3] M. Storchak & T. Stehle, *Untersuchung der thermischen Wirkungen beim orthogonalen Zerspanen*. Institut für Werkzeugmaschinen, Universität Stuttgart.
- [4] E. Uhlmann & J. Hu, Thermal Modelling of a High-Speed Motor Spindle, 5<sup>th</sup> CIRP Conference on High Performance Cutting 2012, (2012), pp. 313-318. <https://doi.org/10.1016/j.procir.2012.04.056>.
- [5] C. Brecher, K. Bakarinos, S. Neus, M. Wennemer & M. Fey, Thermische Simulation von Vorschubachskomponenten. *Wt Werkstattstechnik online*, (2015), pp.156-160. [doi.org/10.37544/1436-4980-2015-03-80](https://doi.org/10.37544/1436-4980-2015-03-80).
- [6] M. Weck, *Werkzeugmaschinen 5 Messtechnische Untersuchung und Beurteilung, dynamische Stabilität*. Springer, (2006).
- [7] M. N. Özisik, H. R.B. Orlande, M.J. Colaco & R. Cotta, *Finite Difference Methods in Heat Transfer*. CRC Press Taylor & Francis Group, (2017).
- [8] K. D. Cole, J.V. Beck, A. H. Sheikh & B. Litkouhi, *Heat Conduction using Green's Functions*. Second Edition. Taylor & Francis Group, LCC, (2011).
- [9] I. Magnabosso, P. Ferro, A. Tiziani, F. Bonollo, Induction heat treatment of a ISO C45 steel bar: Experimental and Numerical Analysis. *Computational Materials Science*, vol. 35, Issue 2, (2006), pp. 98-106. <https://doi.org/10.1016/j.commatsci.2005.03.010>.
- [10] M. Szulborski, S. Lapczynski & L. Kolimas, Thermal Analysis of Heat Distribution in Busbars during Rated Current flow in Low-Voltage Industrial Switchgear. *Energies* 2021, 14, 2427, (2021). <https://doi.org/10.3390/en14092427>.
- [11] P. Bencs, Sz. Szabó & D. Oertel, Simultaneous Measurement of Velocity and Temperature Field in the Downstream region of a Heated Cylinder. *Engineering Review*, vol. 34, Issue 1, pp.7-13, (2014).
- [12] H. Je-Chin & L. M. Wright, *Experimental Methods in Heat Transfer and Fluid Mechanics*. Taylor & Francis Group, CRC Press, (2020).
- [13] S. Seguir-Ouali, D. Saury, S. Harmand, O. Phillipart & D. Laloy, Convective Heat Transfer inside a Rotating Cylinder with an axial Air Flow. *International Journal of Thermal Sciences* 45(2006), pp. 1166-1178, (2006).
- [14] P. Stephan, S. Kabelac, M. Kind, D. Mewes, K. Schaber & T. Wetzel, *VDI-Wärmeatlas, Fachlicher Träger VDI/Gesellschaft, Verfahrenstechnik und Chemieingenieurwesen*. 12 Auflage, Springer Vieweg, (2019). <https://doi.org/10.1007/978-3-662-52989-8>.
- [15] T. L. Bergman, A. S. Lavine, *Fundamentals of Heat and Mass Transfer*. Eight Edition, Wiley & Sons, (2017).